Challenge and adventure: twenty years of searching for the model structure of the polyaniline/camphorsulfonic acid conducting polymer system leading to an artificial intelligence approach[*)]

Tomasz Kozik[1), **)], **Maciej Śniechowski**[1)], **Wojciech Łużny**[1)]

Abstract: The search for the model structure of polyaniline/camphorsulfonic acid (PANI/CSA) began approximately twenty years ago and remained an unsolved problem. Recently, a new molecular dynamics based model was published in which the system forms a structure of alternating double layers. Having brought together all available information regarding the system, an artificial intelligence approach was formulated, which resulted in finding a model of the crystalline regions of the polymer system in agreement with various experimental results. The approach is thoroughly described due to its versatility.

Keywords: polyaniline, X-ray diffraction, modeling, simulations.

Wyzwanie i przygoda: dwadzieścia lat poszukiwań modelu struktury polimerowego systemu przewodzącego polianilina/kwas kamforosulfonowy prowadzących do wykorzystania metod sztucznej inteligencji

Streszczenie: Poszukiwania modelu struktury systemu polianilina/kwas kamforosulfonowy (PANI/CSA) rozpoczęły się przed ok. dwudziestu laty, nadal jednak problem pozostaje nierozwiązany. W minionych latach opublikowano nowy model otrzymany w wyniku symulacji metodą dynamiki molekularnej. Zgodnie z jego przewidywaniami w systemie PANI/CSA powstaje struktura naprzemiennych dwuwarstw. Na podstawie dostępnej wiedzy sformułowano wykorzystującą algorytmy sztucznej inteligencji metodę, która doprowadziła do znalezienia modelu wykazującego zgodność z różnego rodzaju doświadczeniami. Ze względu na uniwersalność opracowanej metody, szczegółowo ją opisano.

Słowa kluczowe: polianilina, dyfrakcja rentgenowska, modelowanie, symulacje.

The conducting polymer system obtained in the process of protonating a form of polyaniline named emeraldine (PANI) with camphorsulfonic acid (CSA), as a compound abbreviated PANI/CSA, has been studied for over twenty years. One of the most noteworthy properties of this system, which attracted a lot of scientific interest during this time span, is its electrical conductivity introduced by the protonation process [1]. Despite being known for such a long time, it is still studied until this day, with research focusing on synthesis methods [2] and

its applications, by itself or as part of a nanocomposite, as a thermoelectric [3] and as a sensor material [4].

Alongside such studies, structural investigations have been carried out, aimed at determining the structure of the crystalline regions of this polymer system. They were initiated in 1997 by a paper [5] in which two models of a crystalline unit cell are presented. X-ray diffraction calculations were performed for both models and the resulting curves were shown to be in good agreement with the crystalline component of a diffraction pattern recorded for a sample considered as a powder one. However, one of the diffraction peaks is described there as a harmonic of a preceding one. This was questioned in [6, 7] where the anisotropy of thin PANI/CSA films was studied. The anisotropy of these two peaks was found to be different, and thus they cannot arise from the same type of ordering and one cannot be a harmonic of the other.

A very different model was published two years later [8]. On a large scale, the molecules in it were organized into a lamellar architecture. Similarly to the earlier mod-

[1)] AGH University of Science and Technology, Faculty of Physics and Applied Computer Science, Al. Adama Mickiewicza 30, 30-059 Krakow, Poland.

[**)] Author for correspondence; e-mail: Tomasz.Kozik@fis.agh.edu.pl

els, this one was supported by X-ray diffraction calculations, which were in good agreement with experiment. However, the reference experimental curve was different than the one used in [5]. This is a recurring problem in structural modeling of PANI/CSA – the experimentally obtained X-ray diffraction patterns for samples are not entirely consistent and may be different for different samples. The differences are primarily in crystalline peak intensity, but also to a small extent in peak position.

Yet another model was published another two years later [9, 10]. This model was different from the previous ones in that it was described more qualitatively and no diffraction profiles were calculated. Its characteristic feature was that PANI chains were separated by a much larger number of CSA counter ions than in previous models.

The next step was an attempt to take advantage of molecular dynamics simulations to aid the modeling process. All of the above described models were tested for stability in such a simulation [11]. However, in these preliminary simulations none of the existing models appeared to be stable – the ordered structure was not preserved.

New, extensive molecular dynamics simulation studies of this system were performed and reported much later [12, 13]. In this case it was found that simulations lead either to a structure with no order, or to a new type of structure of alternating double layers of polymer chains and dopant molecules. This arrangement exhibited a form of long-range ordering and X-ray diffraction calculations described in the cited papers showed a qualitative agreement with the experimental pattern. What is more, this type of structure allowed explaining the structural anisotropy of thin films.

The most recent paper devoted to structural investigation of the PANI/CSA polymer system [14] focuses on describing the neutron diffraction patterns obtained for two types of PANI/CSA samples – a regular one and a partially deuterated one – and how the model of alternating bilayers of the PANI/CSA crystalline structure can be used to explain these differences. For the sake of performing neutron diffraction calculations, an artificial intelligence (AI) approach was used to find a model of the crystalline unit cell of this system. It is worth noting that while the algorithm was aimed at finding a structure reproducing the X-ray diffraction pattern and succeeded, the same unit cell is valid for neutron diffraction calculations. This is the basis for the conclusion that the alternating bilayer model is supported by all so far known investigation techniques.

The aim of this paper is to provide an insight into the artificial intelligence approach used in [14]. Because the approach was in the end successful, it is worth recapitulating and elaborating on all the steps directly taken and surrounding this method. Possibly, a very analogous course of action might be again successful in solving the structure of other polymer systems in future, since several steps which were taken may be regarded as universal.

METHODOLOGY

Available information regarding PANI/CSA

Although at first a seemingly straightforward statement, the chemical composition of samples was known. Partially crystalline ones may be obtained by protonating polyaniline in a racemic mixture of CSA, that is containing an equal amount of its two chiral enantiomers. This impacts the modeling procedure, as it must take both of these structures of CSA into account and answer the question if the differences between them impact the structure of the compound and how. This knowledge also allowed assuming the average bond lengths between individual atoms and indicating which fragments of the structure are rigid and which are flexible.

As it was mentioned in the introductory part, the X-ray diffraction pattern may vary between different PANI/CSA samples. However, for a properly prepared powder sample of the compound, five diffraction peaks should be observed for scattering angles equal to approximately 5°, 10°, 15°, 20° and 25° (CuK_α source). As a reference pattern in the reported procedure, the crystalline component of the full PANI/CSA diffraction profile from [5] was used. However, while the measured sample was regarded as a powder one, there was most probably a preferred orientation introduced. A correction factor calculated from the patterns reported in [14] with a value of 0.5245 was used to scale the overestimated peak. Such a representative crystalline component is depicted in Fig. 1.

A very important source of information was the structural anisotropy of thin films, revealing itself for instance in synchrotron radiation grazing incident beam surface diffraction reported in [15]. The diffraction peaks calculated for a model structure cannot contradict these mea-
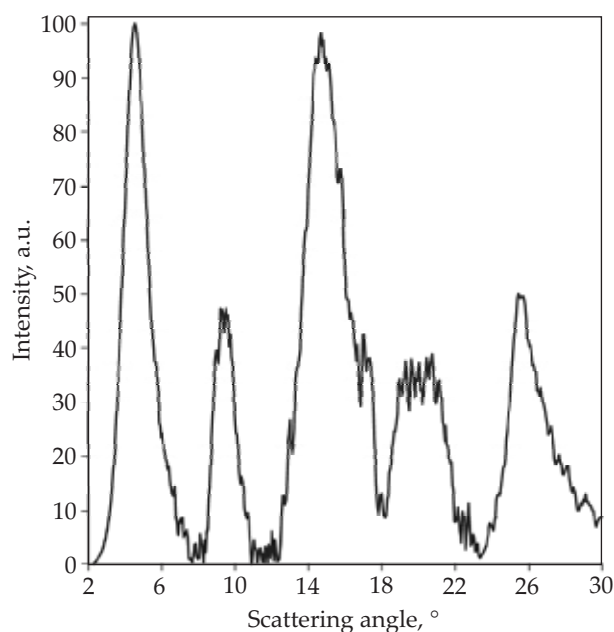

Fig. 1. A representative crystalline component of a PANI/CSA diffraction pattern

surements, *i.e.*, one peak cannot be the harmonic of another one if they have different anisotropy. What is more, these results suggest the peak indexing, as they allow identifying peaks related to nearly orthogonal directions.

The results of molecular dynamics simulations reported in [12, 13] also provided a point of reference. While the scope of the artificial intelligence modeling was prepared in a way which would allow taking into account a structure of alternating bilayers anyhow, the results of these simulations confirmed that this was the correct approach. Furthermore, once a model of the unit cell is found by the AI, it could be tested for stability in a molecular dynamics simulation.

The neutron diffraction results, published only recently in [14], but available while the modeling was in progress, were yet another important source of information. Even if the model is optimized with respect to X-ray diffraction profiles, the neutron diffraction profiles calculated for it should at least not contradict experimental results.

Determining the scope of the modeling

The first step in the artificial intelligence approach was determining the scope of the modeling, that is what part of the available data on PANI/CSA can be directly used for determining what kind of parameters should be searched for by an optimizer.

The insight provided by the surface diffraction experiments [15] suggested that the first, second, and fifth diffraction peaks arise from ordering in three perpendicular directions. Hence it was reasonable to assume that the edges of a crystalline unit cell should be of length *ca.* 20 Å, 9.3 Å and 3.5 Å, respectively. Because for thin films the second peak is visible only in transmission diffraction geometry, it was straightforward to assume that it is related to the ordering along polymer chains, which cannot be perpendicular to the plane of a very thin sample. Indeed, 9.3 Å corresponds to the approximate length

of two aniline units building the polymer chain. The interplanar length of 3.5 Å was initially assumed to correspond to aromatic ring stacking within the sample due to its value. Finally, the question of the origin of the long period had to be addressed. A simple alternating ordering of PANI chains and CSA counter ions, assumed originally in [5], could not fit to this period due to the fact that it physically occupies too little space. Hence by means of purely geometric speculation it was assumed that the layout is doubled, that is that there exists perhaps a structure of alternating double layers of chains and double layers of dopant molecules. The last issue which must be accounted for is the chirality of CSA. To model a double bilayer structure and to include two CSA enantiomers within a unit cell, it was assumed that the unit cell exhibits inversion symmetry.

Alongside initial attempts at modeling described above, molecular dynamics simulations were being carried out. As it was reported in [12, 13], it was found that a structure of alternating bilayers is stable and yields a diffraction pattern which approximately and qualitatively fits to the experimental one. While these results on one hand strengthened the presumption that such a structure is indeed present in PANI/CSA, on the other they influenced the modeling scope. So far, the optimizers were assuming that the fifth peak should be indexed (010) and the aromatic ring stacking is of the most simple "sandwich" type, while the molecular dynamics simulations suggested that it should be indexed as (020), the unit cell edge should be assumed to be twice as long as in the initial modeling, and that the stacking type may not necessarily be of the "sandwich" type, but could be of the "parallel-displaced" or even "t-shaped" type. The question of the presence of the last type of stacking was answered negatively after some calculations, because it could not lead to diffraction yielding a fifth peak of substantial intensity.

Knowledge of the chemical composition of samples allowed simplifying the modeling procedure from search-

T a b l e 1. Parameters of the model

Symbol(s)	Description	Commentary
$a, b, c, \alpha, \beta, \gamma$	Unit cell parameters	The first three may be calculated from the other ones if they are constrained to produce specified interplanar distances.
$\Delta a_{PANI}, \Delta b_{PANI}, \Delta c_{PANI}$	PANI chain position	The first two define the point at which the chain axis enters the cell, the third defines the offset of all atoms along this axis. These are fractions of respective unit cell lengths.
φ_{PANI}	PANI chain rotation about its axis	Chain axis is aligned parallel to *c*.
τ_{RING}	Torsion angle of the aromatic rings in the chain	Consecutive rings rotate in opposite directions.
$\Delta a_{CSA}, \Delta b_{CSA}, \Delta c_{CSA}$	CSA counter ion position	These are fractions of respective unit cell lengths.
$\varphi_{CSA}, \theta_{CSA}, \tau_{CSA}$	CSA counter ion orientation	C–S bond axis is aligned parallel to *c* if these angles are 0.
τ_1	CSA internal torsion angle – rotation about S–C bond	–
τ_2	CSA internal torsion angle – rotation of the rigid part about the C–C bond	–

ing for positions of individual atoms within the unit cell to searching for the positions and orientations of selected rigid building blocks within the cell and the relative orientations of the other building blocks. Furthermore, the number of parameters was greatly reduced by specifying that the polymer chain must be adjusted to one of the unit cell edges in the sense that it must continue through consecutive unit cells in this direction (chosen cell axis c).

Finally, the number of unit cell parameters could be even further reduced by applying constraints on the cell edge lengths *a*, *b* and *c* by calculating them from cell angle values and fixed interplanar distances d_{100}, d_{020} and d_{001} (or only one or two of them). This however limits the flexibility of the optimizer.

To summarize, all the relevant parameters which need to be found by an optimizer are described in Table 1.

Verification methods

While an optimization algorithm may succeed in finding a layout of atoms within a unit cell which produces a calculated diffraction pattern in good agreement with the experimental one, the result needs to be verified before accepting it as a new model. Primarily, the model needs to be inspected for general plausibility. Solutions which include major collisions of atoms or large empty spaces for which no interaction justifying their formation can be specified cannot be further considered. Afterwards, the model can be checked against selected experimental and simulation data not necessarily used in specifying the model scope.

First of them would be, apparently, grazing incident beam data. While they were used in the construction of the model scope, the optimizer could have found a way to bypass the imposed rules for the main crystalline reflections. An actual example is a case in which the second peak which is supposed to be (001) and most certainly not (200), as was discussed in the introductory part, was designated as a composition of these two with almost equal intensity contribution. This was overcome only after explicitly reducing the goodness of fit of those models in which the intensity of the (200) peak was high. Additionally, grazing incident beam experiments provided some information concerning the two remaining peaks (third and fourth), not yet used in the formulation of the model. Namely, the third peak should be of mixed indices (ordering in a direction acute to a thin sample plane) and the fourth one should be composed of several reflexes, not having a preferred orientation. The model found by the optimizer should not contradict these findings.

The second could be molecular dynamics simulations. The structure found by the optimizer could be used as input for a small scale simulation in order to check its stability. If it does not undergo major changes in such a simulation, it can be considered stable.

Finally, there are the results of neutron diffraction experiments, reported thoroughly in [14]. It would be a ma-jor argument for the validity of the found model if it could explain the differences observed between the curves recorded for regular and partially deuterated PANI/CSA samples. This would require altering the structure by substituting hydrogen with deuterium in appropriate places and calculating a neutron diffraction pattern before and after such a substitution. If these two curves are related at least qualitatively in the same way as the appropriate experimental ones, there is an agreement.

The optimization algorithm

The artificial intelligence refinement procedure used for searching for a model structure was a so-called swarm intelligence kind of method. It was based primarily on the firefly algorithm [16] with a special treatment of the influence of the best model in a given collection on the other models and with values of algorithm parameters depending on iteration number.

The crystalline component of the full X-ray diffraction profile was chosen as reference data for the optimizer – it was tasked with finding a structure which produces a diffraction pattern as similar to that one as possible.

The parameters listed in Table 1 with their variation range span the solution space of the problem being solved. A point in this space defines a model completely. Therefore, each possible solution is associated with a position vector in this space, which in turn corresponds to a position of an abstract firefly within a unit hypercube. It suffices to model each position vector component in a range from 0 to 1 because it can be converted to an actual parameter value by means of a linear function, taking into account the variation range for that specific parameter. It also removes the potential problem of large differences in variation ranges of the parameters. Each abstract firefly also possesses a velocity vector. Upon hitting the side of the hypercube, the firefly literally bounces off of it.

At the beginning of the algorithm, the positions of a fixed number of fireflies are randomly assigned. Initially, the fireflies are motionless. The algorithm performs a fixed number of iterations, in which new velocities are calculated and the positions are updated according to these velocities. Additionally, the positions are altered by adding a vector of random numbers from the Cauchy distribution multiplied by a parameter *D*. This greatly raises the efficiency of searching through the solution space and also can spontaneously generate fireflies positioned in previously unexplored areas of the hypercube.

The velocity calculation procedure is the most complex part of an iteration. A new velocity for each given firefly is calculated as a sum of the old velocity multiplied by an always smaller than 1 number ω, representing the inertia of the firefly, and a computed interaction vector, which is for each firefly a sum of three vectors.

The first interaction vector is the attractive interaction between fireflies with the exclusion of the best one in the current collection. The metaphor of the original formula-

tion from [16] is that each firefly emits light signals proportional to the quality of the solution it represents and is attracted to all the fireflies brighter than itself. Additionally, this attractive force exponentially weakens with distance. This is a crucial idea – thanks to this, the fireflies can divide into groups swarming near different optima of the problem being solved, since interactions keeping the sub-swarms together are stronger than the interactions with other sub-swarms. For each pair of fireflies in the positions (vectors) x_i (the one being attracted) and x_j (the brighter one), an interaction vector of the form

$$\beta\left(x_j - x_i\right) e^{-\gamma\left|x_j - x_i\right|} \tag{1}$$

is added to the velocity, where γ and β are parameters of the algorithm. The value of γ does not change in the course of the algorithm. Additionally, such a formula does not produce unreasonably strong interactions between fireflies which are very close to each other.

The interaction term for each firefly caused by attraction by the best one in the collection (in the current iteration) is treated slightly differently – the parameter β is replaced by a φ_g parameter, which changes differently. Otherwise, the formula is the same.

Finally, each firefly keeps record of its best known position in the history of its movement. It is very slightly repulsed from this position, to improve the searching capability of the algorithm. This interaction is scaled with the parameter φ_l.

The values of the parameters D, ω, β and φ_l linearly decrease in their value with the iteration number, to zero, except ω, which tends to a constant value. Contrarily, the
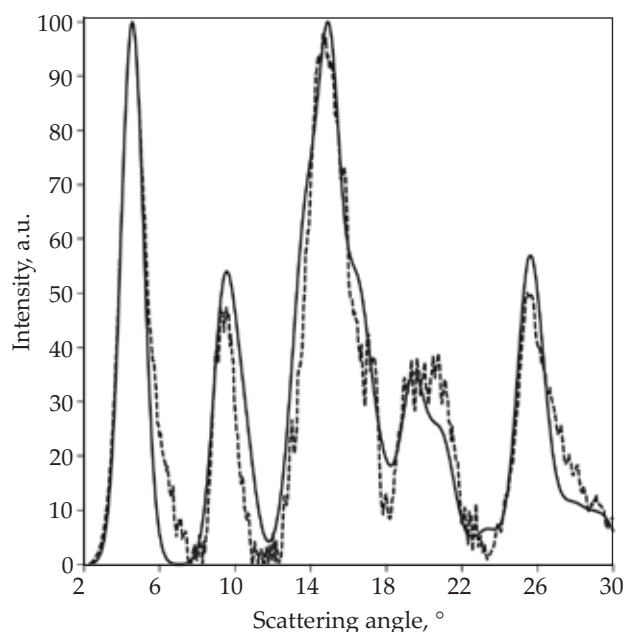

Fig. 2. The diffraction pattern calculated for the model (solid) compared to the reference crystalline component (dashed)

value of φ_g increases linearly with the iteration number. This means that the behavior of the algorithm changes in time – initially, it performs a thorough search of the solution space, then the fireflies start swarming near found local optima, and near the end of the algorithm converge to the optima.

RESULTS AND DISCUSSION

The best model found by the optimizer is described in [14]. The values of the parameters listed in Table 1 found by the optimizer are reported in Table 2. The diffraction curve calculated for this model, along with the (corrected) experimental crystalline component of the PANI/CSA diffraction pattern, are plotted together in Fig. 2.

Regarding verification methods described earlier, this model passes all of these tests. The main diffraction peaks are properly indexed, the third diffraction peak is formed primarily by reflexes (210) and (2-10), which fits the predicted anisotropy, and the fourth peak is composed of several reflexes, not giving it a characteristic anisotropy. The model is stable in small-scale molecular dynamics simulations and allows reproducing the differences between experimental neutron diffraction patterns, as it was thoroughly reported in [14].

CONCLUSIONS

To summarize, in this paper the methodology used to find the recently published new structural model of the PANI/CSA conducting polymer system was reviewed and thoroughly described. Available data regarding the investigated system were separated into data used for the construction of a solution space, data used for verification of the model and data directly used as reference in the

T a b l e 2. Model parameter values found by the optimizer

Parameter	Value
a	19.4417 Å
b	7.2044 Å
c	9.6428 Å
α	103.57°
β	88.45°
γ	95.15°
Δa_{PANI}	0.1372
Δb_{PANI}	0.2424
Δc_{PANI}	0.2299
φ_{PANI}	178.69°
τ_{RING}	2.74°
Δa_{CSA}	0.2756
Δb_{CSA}	0.6875
Δc_{CSA}	-0.2121
φ_{CSA}	31.74°
θ_{CSA}	53.65°
τ_{CSA}	146.89°
τ_1	58.63°
τ_2	264.64°

structural modeling. The algorithm used for the modeling (search) was based on the firefly algorithm with parameters varying with iteration number. Hopefully, this approach could be in future applied to other structural problems.

REFERENCES

[1] Epstein A.J., Ginder J.M., Zuo F. *et al.*: *Synthetic Metals* **1987**, *21*, 63.
http://dx.doi.org/10.1016/0379-6779(87)90067-1
[2] Zhou Y., Wang Y., He D. *et al.*: *Journal of Nanoscience and Nanotechnology* **2014**, *14*, 3417.
http://dx.doi.org/10.1166/jnn.2014.7959
[3] Anno H., Hokazono M., Akagi F. *et al.*: *Journal of Electronic Materials* **2013**, *42*, 1346.
http://dx.doi.org/10.1007/s11664-012-2368-z
[4] Pang Z., Fu J., Lv P. *et al.*: *Sensors* **2014**, *14*, 21 453.
http://dx.doi.org/10.3390/s141121453
[5] Łużny W., Samuelsen E.J., Djurado D., Nicolau Y.F.: *Synthetic Metals* **1997**, *90*, 19.
http://dx.doi.org/10.1016/S0379-6779(97)03908-8
[6] Bańka E., Łużny W.: *Synthetic Metals* **1999**, *101*, 715.
http://dx.doi.org/10.1016/S0379-6779(98)01151-5
[7] Łużny W., Bańka E.: *Macromolecules* **2000**, *33*, 425.
http://dx.doi.org/10.1021/ma9913663
[8] Winokur M.J., Guo H., Kaner R.B.: *Synthetic Metals* **2001**, *119*, 403.
http://dx.doi.org/10.1016/S0379-6779(00)01130-9
[9] Jana T., Roy S., Nandi A.K.: *Synthetic Metals* **2003**, *132*, 257. http://dx.doi.org/10.1016/S0379-6779(02)00454-X
[10] Jana T., Chatterjee J., Nandi A.K.: *Macromolecular Symposia* **2003**, *203*, 47.
http://dx.doi.org/10.1002/masy.200351304
[11] Łużny W., Djurado D., Johnson M.R. *et al.*: "Computer simulations of the structural properties of conducting polymers: the review of some recent results", Proceedings of the International Conference on Science and Technology of Synthetic Metals, Dublin, Ireland, July 2–7, 2006, W10.
[12] Śniechowski M., Borek R., Piwowarczyk K., Łużny W.: *Macromolecular Theory and Simulations* **2015**, *24*, 284. http://dx.doi.org/10.1002/mats.201400105
[13] Śniechowski M., Kozik T., Niedźwiedź W., Łużny W.: *Macromolecular Theory and Simulations* **2016**, *25*, 328.
http://dx.doi.org/10.1002/mats.201600010
[14] Kozik T., Śniechowski M., Łużny W. *et al.*: *Polymer* **2017**, *111*, 148.
http://dx.doi.org/10.1016/j.polymer.2017.01.034
[15] Łużny W., Samuelsen E.J., Breiby D.W.: *Fibres & Textiles in Eastern Europe* **2003**, *11*, 97.
[16] Yang X.-S., He X.: *International Journal of Swarm Intelligence* **2013**, *1*, 36.

Received 30 III 2017.

*Najlepsze życzenia
Szczęśliwego Nowego Roku 2018
Czytelnikom, Autorom
i Współpracownikom
składa Redakcja*